



**HAL**  
open science

## Uncertainty analysis and validation of the estimation of effective hydraulic properties.

Arnaud Mesgouez, Samuel Buis, Stéphane Ruy, Gaëlle Lefeuvre-Mesgouez

► **To cite this version:**

Arnaud Mesgouez, Samuel Buis, Stéphane Ruy, Gaëlle Lefeuvre-Mesgouez. Uncertainty analysis and validation of the estimation of effective hydraulic properties.. 2013. hal-00793526v3

**HAL Id: hal-00793526**

**<https://hal.science/hal-00793526v3>**

Preprint submitted on 18 Oct 2013 (v3), last revised 24 Mar 2014 (v4)

**HAL** is a multi-disciplinary open access archive for the deposit and dissemination of scientific research documents, whether they are published or not. The documents may come from teaching and research institutions in France or abroad, or from public or private research centers.

L'archive ouverte pluridisciplinaire **HAL**, est destinée au dépôt et à la diffusion de documents scientifiques de niveau recherche, publiés ou non, émanant des établissements d'enseignement et de recherche français ou étrangers, des laboratoires publics ou privés.

Manuscript Number:

Title: Uncertainty analysis and validation of the estimation of effective hydraulic properties at the Darcy scale

Article Type: Research Paper

Keywords: effective hydraulic parameters  
heterogeneous porous media  
uncertainty estimation  
green roof substrate  
the Richards equation  
bootstrapping method

Corresponding Author: Dr. Arnaud Mesgouez, Ph. D.

Corresponding Author's Institution: Universite d'Avignon et des Pays de Vaucluse

First Author: Arnaud Mesgouez, Ph. D.

Order of Authors: Arnaud Mesgouez, Ph. D.; Samuel Buis, Ph. D.; Stéphane Ruy, Ph. D.; Gaëlle Lefeuvre-Mesgouez, Ph. D.

Abstract: The determination of the hydraulic properties of heterogeneous soils or porous media remains challenging. In the present study, we focus on determining the effective properties of heterogeneous porous media at the Darcy scale with an analysis of their uncertainties.

Preliminary, experimental measurements of the hydraulic properties of each component of the heterogeneous medium are obtained. The properties of the effective medium, representing an equivalent homogeneous material, are determined numerically by simulating a water flow in a three-dimensional representation of the heterogeneous medium, under steady-state scenarios and using its component properties. One of the major aspects of this study is to take into account the uncertainties of these properties in the computation and evaluation of the effective properties. This is done using a bootstrap method.

Numerical evaporation experiments are conducted both on the heterogeneous and on the effective homogeneous materials to evaluate the effectiveness of the proposed approach. First, the impact of the uncertainties of the component properties on the simulated water matric potential is found to be high for the heterogeneous material configuration. Second, it is shown that the strategy developed herein leads to a reduction of this impact. Finally, the adequacy between the means of the simulations for the two configurations confirms the suitability of the homogenization approach, even in the case of dynamic scenarios.

The methodology proposed in this study is generic. It is applied to green roof substrates, a two-component media composed of bark compost and pozzolan, used in the construction of buildings.

Suggested Reviewers: Paolo Nasta  
Department of Earth and Atmospheric Sciences, University of Nebraska, Lincoln

paolo.nasta@unina.it

Competent at doing the review because of its research activities which include the scope of the proposed manuscript.

Harrie-Jan Hendricks Franssen

Forschungszentrum Jülich IBG-3, Wilhelm-Johnen-Straße, 52428 Jülich, Germany

h.hendricks-franssen@fz-juelich.de

Competent at doing the review because of its research activities which include the scope of the proposed manuscript.

DongHao Ma

State Experimental Station of Agro-Ecosystem in Fengqiu, State Key Laboratory of Soil and Sustainable Agriculture, Institute of Soil Science, Chinese Academy of Sciences, Nanjing 210008, China

dhma@issas.ac.cn

Competent at doing the review because of its research activities which include the scope of the proposed manuscript.

Thierry Mara

Faculté des Sciences, laboratoire PIMENT, Université de la réunion, France

mara@univ-reunion.fr

Competent at doing the review because of its research activities which include the scope of the proposed manuscript.

Mathieu Javaux

Earth and Life Institute Université catholique de Louvain, Louvain-la-Neuve, B-1348 Belgium

mathieu.javaux@uclouvain.be

Competent at doing the review because of its research activities which include the scope of the proposed manuscript.

Dr. A. Mesgouez  
Université d'Avignon, Faculté des Sciences  
UMR1114 EMMAH  
33 rue Louis Pasteur, F-84000 Avignon  
e-mail: arnaud.mesgouez@univ-avignon.fr  
Tel.: +33(0)4 90 14 44 63

October 10, 2013

Dear Pr. A. Bárdossy,

We are pleased to submit our new manuscript entitled: “ Uncertainty analysis and validation of the estimation of effective hydraulic properties at the Darcy scale ” to Journal of Hydrology.

The manuscript deals with the determination of the effective hydraulic properties of real heterogeneous materials. Simulations of water flow in heterogeneous and effective media at the Darcy scale have been performed using a C++ three-dimensional parallelized code. The first objective of this study is to take into account the uncertainties of the hydraulic properties of each individual component in the computation and evaluation of the effective properties. The second objective is to evaluate the effectiveness of our homogenization approach with respect to dynamic simulations. The methodology proposed in this study is generic. It was applied here to green roof substrates, a two-component media composed of bark compost and pozzolan, used in the construction of buildings. The two main results presented in the manuscript can be summarized as follows:

- A good adequacy between the means of the simulated water matric potentials for the heterogeneous and effective materials is obtained in the case of dynamic evaporation scenarios.
- A reduction in the level of uncertainties is obtained for the effective hydraulic properties.

This paper is original, and it has not been submitted elsewhere.

Hoping that this contribution will interest you.

Sincerely Yours,

A. Mesgouez, S. Buis, S. Ruy, G.  
Lefeuvre-Mesgouez.

Highlights:

- The effective hydraulic properties of real heterogeneous media were evaluated at the Darcy scale.
- The suitability of the homogenization approach was shown in a case of dynamic evaporation simulations.
- We accounted for the uncertainties for the hydraulic properties of each material.
- A reduction in the level of uncertainties was obtained for the effective hydraulic properties.

# Uncertainty analysis and validation of the estimation of effective hydraulic properties at the Darcy scale

A. Mesgouez<sup>a,b,\*</sup>, S. Buis<sup>b,a</sup>, S. Ruy<sup>b,a</sup>, G. Lefeuvre-Mesgouez<sup>a,b</sup>

<sup>a</sup>*Université d'Avignon et des Pays de Vaucluse, UMR1114 EMMAH, Faculté des Sciences, F-84000 Avignon, France*

<sup>b</sup>*INRA, UMR1114 EMMAH, F-84914 Avignon, France*

---

## Abstract

The determination of the hydraulic properties of heterogeneous soils or porous media remains challenging. In the present study, we focus on determining the effective properties of heterogeneous porous media at the Darcy scale with an analysis of their uncertainties.

Preliminary, experimental measurements of the hydraulic properties of each component of the heterogeneous medium are obtained. The properties of the effective medium, representing an equivalent homogeneous material, are determined numerically by simulating a water flow in a three-dimensional representation of the heterogeneous medium, under steady-state scenarios and using its component properties. One of the major aspects of this study is to take into account the uncertainties of these properties in the computation and evaluation of the effective properties. This is done using a bootstrap method.

---

\*Corresponding author

*Email addresses:* [arnaud.mesgouez@univ-avignon.fr](mailto:arnaud.mesgouez@univ-avignon.fr) (A. Mesgouez),  
[sbuis@avignon.inra.fr](mailto:sbuis@avignon.inra.fr) (S. Buis), [ruy@avignon.inra.fr](mailto:ruy@avignon.inra.fr) (S. Ruy),  
[gaelle.mesgouez@univ-avignon.fr](mailto:gaelle.mesgouez@univ-avignon.fr) (G. Lefeuvre-Mesgouez)

Numerical evaporation experiments are conducted both on the heterogeneous and on the effective homogeneous materials to evaluate the effectiveness of the proposed approach. First, the impact of the uncertainties of the component properties on the simulated water matric potential is found to be high for the heterogeneous material configuration. Second, it is shown that the strategy developed herein leads to a reduction of this impact. Finally, the adequacy between the means of the simulations for the two configurations confirms the suitability of the homogenization approach, even in the case of dynamic scenarios.

The methodology proposed in this study is generic. It is applied to green roof substrates, a two-component media composed of bark compost and pozzolan, used in the construction of buildings.

*Keywords:* effective hydraulic parameters, heterogeneous porous media, uncertainty estimation, green roof substrate, the Richards equation, bootstrapping method

---

## 1. Introduction

At the Darcy scale, heterogeneous media can be represented in different ways. A detailed description of the various representations can be found in the reviews of Renard and de Marsily (1997) or Vereecken et al. (2007). Basically, the heterogeneous medium can be modeled with a spatial distribution of properties inside a single unit, see Vogel et al. (2010) among others, or with a patchwork of homogeneous sub-units, see Samouëlian et al. (2011) for example. These sub-units can be artificial ones obtained from several calibrated sands (Danquigny and Ackerer, 2005), or natural units defined from

10 pedological characterization (Ma et al., 2010; Samouëlian et al., 2011). The  
11 approach proposed in this article refers to the second way of representation.  
12 In this case, each component of the heterogeneous medium is considered as a  
13 single-phase continuum, the properties of which are defined by macroscopic  
14 parameters (hydraulic conductivity and water retention curves) and by phe-  
15 nomenological laws (the Darcy law and the Richards equation). Water flow  
16 simulation or water balance computation can be performed on an elementary  
17 volume by using a numerical solver of the Richards equation accounting for  
18 the spatial heterogeneity of the hydraulic properties. The spatial structure  
19 must be known to distribute the hydraulic properties of each material on the  
20 volume of interest. Solving the Richards equation is very tedious, in this case,  
21 since it is a non linear equation applied to a multidimensional geometry. A  
22 simpler approach consists in replacing the explicit three-dimensional struc-  
23 ture of the heterogeneous volume by a homogeneous medium, the properties  
24 of which take into account the hydraulic properties of each material, in such  
25 a way that simulations conducted on both domains produce similar bound-  
26 ary water fluxes under identical boundary Dirichlet conditions (Samouëlian  
27 et al., 2011). Such a medium and such properties are known, respectively, as  
28 an effective medium and effective properties.

29 The first objective of this study is to characterize the effective hydraulic  
30 properties of a real material taking into account uncertainties in the deter-  
31 mination of the hydraulic properties of its individual components. Due to  
32 the recent advances in computing capabilities, numerical approaches are now  
33 widely used for the determination of effective properties (Samouëlian et al.,  
34 2007; Vogel et al., 2010). Studies carried out on natural soils are proposed

35 by Vogel and Roth (1998), Javaux and Vanclooster (2006) or Samouëlian et  
36 al. (2011). These authors estimate the effective hydraulic properties of Al-  
37 beluvisol, agricultural silt soil or monolithic subsoil, respectively, but do not  
38 integrate a complete uncertainty evaluation in their studies. However, the  
39 process of estimating the hydraulic properties of a given material includes  
40 various sources of uncertainties (Mohrath et al., 1997; Peters and Durner,  
41 2008). They may significantly affect numerical simulations (Christiaens and  
42 Feyen, 2001; Coppola et al., 2009; Pan et al., 2009) and thus affect the  
43 estimation of effective properties or their evaluation using dynamic scenar-  
44 ios. Therefore, estimating the resulting uncertainties of hydraulic properties  
45 and their impacts on simulation results is important to assess the quality  
46 of effective properties estimation and to interpret the results. Taking into  
47 account all type of uncertainties, using for example Monte Carlo error prop-  
48 agation method, would be very tedious and difficult since they are numerous  
49 and since modeling their probability distribution, including possible depen-  
50 dencies, would be extremely complicated. The bootstrap method is a re-  
51 sampling method which is recognized to be a simple and efficient way to esti-  
52 mate the probability distribution of a statistic. It can be used to estimate a  
53 statistic without it being biased, to evaluate the accuracy of this estimation  
54 and/or to build confidence intervals for this statistic (Efron and Tibshirani,  
55 1994; Manly, 2006). Here, we propose to use this method for evaluating the  
56 uncertainties of the effective hydraulic properties of a real heterogeneous ma-  
57 terial by taking into account, in the numerical processing, the uncertainties  
58 estimated for the hydraulic properties of each one of its components.

59 The second objective of this study is to evaluate the effectiveness of the

60 proposed approach with respect to dynamic simulations. Several authors  
61 (Vogel et al., 2008; Vogel et al., 2010) note that simulations conducted using  
62 effective parameters may differ from simulations conducted with spatially  
63 distributed parameters. An evaluation of the methodology used to obtain  
64 the effective parameters would, therefore, be required. In the present work,  
65 simulations of a dynamic evaporation process using either the heterogeneous  
66 medium or the effective homogeneous material are compared. The simula-  
67 tions are performed by including uncertainties estimated for the hydraulic  
68 properties of both the heterogeneous and the effective homogeneous materi-  
69 als, and the impact of these uncertainties are compared.

70 In this study, the methodology is applied to green roof substrates, here-  
71 after called substrate or complex substrate, which is a composite of com-  
72 pressible materials, namely organic matter (bark compost) used as fertilizer,  
73 and of aggregates of volcanic rock (pozzolan) used as rigid skeleton. This  
74 two-component material is considered to serve a number of beneficial pur-  
75 poses that can help in the management of various environmental problems,  
76 such as the reduction of air pollution or of the carbon footprints of cities, the  
77 improvement of storm water management and, of course, the improvement  
78 of energy efficiency in buildings.

79 The manuscript is structured as follows. In section 2, methodologies to  
80 evaluate the hydraulic properties of each component of the substrate, as well  
81 as their associated uncertainties, are stated. Section 3 presents the numerical  
82 tools used to obtain the effective hydraulic properties of the heterogeneous  
83 medium and the uncertainties associated with these properties. Parameter  
84 and uncertainty values relative to the effective material are discussed. Sim-

85 ulation results of dynamic evaporations of the two-component substrate and  
86 the effective medium are compared in section 4. Finally, concluding remarks  
87 and future research perspectives are briefly outlined in section 5.

## 88 **2. Estimation of individual material properties and associated un-** 89 **certainties from experimental measurements**

90 The green roof substrate under study is composed of a combination of  
91 bark compost and pozzolan. Water retention and hydraulic conductivity  
92 are measured for both materials using ad hoc experimental procedures for  
93 different water matric potential and on different samples (please refer to the  
94 Appendix for more details). These hydraulic properties are then modeled by  
95 fitting parametric models to these experimental data. The method used to  
96 assess the associated uncertainties is described in the following subsections  
97 as well as the results obtained. The followed procedure is summarized in Fig.  
98 1, step 1.

### 99 *2.1. Uncertainty evaluation methodology*

100 Various approximations and errors can be sources of uncertainty when  
101 estimating the hydraulic properties of a material. The following typology is  
102 proposed to classify these sources of uncertainty

- 103 1. Variability in the properties of samples: owing to the variability of the  
104 material samples used in some experiments, or to the fact that some  
105 experiments result in the destruction of the samples, measurements of  
106 the properties of a material are often replicated using several samples.  
107 The number of samples may have a significant impact on the estimation

- 108 of the hydraulic properties of a material depending on the level of their  
109 individual variability,
- 110 2. Errors in experimental data due to (i) approximations performed for  
111 instance on length, weight or density measurements, or on transducer  
112 locations, and to (ii) digitalization errors associated with digital data-  
113 loggers. These errors can propagate in the estimation of the hydraulic  
114 properties as noted by Tamari et al. (1993),
  - 115 3. Model errors due to inadequate model assumptions. Vogel et al. (2010)  
116 show in a numerical case study that the validation of the homogeniza-  
117 tion process required a highly flexible hydraulic law model,
  - 118 4. Fitting errors: in the event of a low number of experimental data, the  
119 level of uncertainty of the obtained parameters using parametric models  
120 fitted to the experimental data may be very high, even in case of slight  
121 variability in the properties of the samples and of slight measurement  
122 errors.

123 We use the bootstrap method (Efron and Tibshirani, 1994; Manly, 2006)  
124 to estimate the resulting uncertainties on the hydraulic properties and to  
125 evaluate their impacts on the simulation results. This method can be used  
126 to estimate a statistic without it being biased, to evaluate the accuracy of  
127 this estimation and/or to build confidence intervals for this statistic. In  
128 the present study, the statistics computed are the parameters of the models  
129 describing hydraulic properties. The principle of non-parametric bootstrap-  
130 ping is briefly described hereafter. Let us consider the observation sample  
131 obtained for the computation of the statistic, in our case a set of water re-  
132 tention or conductivity measurements.  $N$  artificial samples, of the same size

133 as the original observation sample, are created by sampling in it with re-  
 134 placement. They are called bootstrap samples. The value of the statistic  
 135 is computed for each one of these bootstrap samples. Its probability distri-  
 136 bution is then approximated using the histogram of its  $N$  computed values.  
 137 In other words, the actual variability of the statistic is estimated using the  
 138 observed variability of all the samples obtained by re sampling. Of course,  
 139 this kind of methodology does not take into account the problem of model  
 140 error, of large biases or of samples non representative of the population. Nev-  
 141 ertheless, it produces accurate descriptions of uncertainties under reasonable  
 142 assumptions and a lower bound of the actual uncertainty level.

143 In the following, the values of the parameters of the hydraulic models are  
 144 estimated by fitting these models on all the available observations. These fits  
 145 are performed using non-linear least squares regression with a trust-region-  
 146 reflective minimizer (Coleman and Li, 1996). Then, the uncertainty distri-  
 147 butions of these parameters are approximated by fitting the models  $N$  times  
 148 on bootstrap samples of the observations. The number of bootstrap samples  
 149 used is always set to  $N = 500$  and their size are the same as the original  
 150 observation sample.

## 151 2.2. *Water retention curves and associated uncertainties*

152 The van-Genuchten model (van Genuchten, 1980) is fitted to the exper-  
 153 imental data to obtain the water retention curve, i.e. the relation between  
 154  $\theta(h, \mathbf{x}, t)$  [ $L^3.L^{-3}$ ], the volumetric water content, and  $h(\mathbf{x}, t)$  [ $L$ ], the water  
 155 matric potential, as follows

$$\theta(h, \mathbf{x}, t) = \theta_r + (\theta_s - \theta_r) \times \left[ 1 + \left( \frac{h(\mathbf{x}, t)}{h_e} \right)^n \right]^{-m} \quad (1)$$

156 where  $\mathbf{x}$  [L] are the spatial coordinates,  $t$  [T] is the time,  $\theta_r$  [ $L^3.L^{-3}$ ] is  
157 the residual volumetric water content,  $\theta_s$  [ $L^3.L^{-3}$ ] is the water content at  
158 saturation,  $h_e$ [L] is a scale parameter,  $n$  [-] and  $m$  [-] are shape parameters  
159 with  $m = 1 - 1/n$ .

160 The resulting uncertainty distributions of the water retention for pozzolan  
161 and compost are presented in Figs. 2. The estimated values of the van  
162 Genuchten model parameters for compost and pozzolan, and the standard  
163 deviations of the associated uncertainty distributions, are displayed in Table  
164 1.

165 The water retention measurements of pozzolan are widely spread near  
166 saturation. High standard deviations for water content,  $0.13 \text{ m}^3/\text{m}^3$  to  $0.14$   
167  $\text{m}^3/\text{m}^3$ , are obtained for matric potential values greater than  $-10^{-2}$  m. They  
168 decrease to a typical value of  $0.03 \text{ m}^3/\text{m}^3$  in the central part of the water  
169 retention curve and are lower to  $0.007 \text{ m}^3/\text{m}^3$  for  $h < -10$  m. According to  
170 the Jurin law, water content near saturation is determined by the proportion  
171 of larger pores (up to 1 mm in diameter) that can be found in pozzolan  
172 aggregates. Due to the small size of the aggregates (diameter of about 5  
173 mm) used in the present study, the proportion of macro pores is highly  
174 variable from one aggregate to the other, which explains the high variability  
175 of the water content near saturation. For lower matric potential values, the  
176 water content variability of pozzolan aggregates may be attributed to factors  
177 involved in the pozzolan formation. Indeed, pozzolan is a porous siliceous  
178 pyroclastic rock, the porosity of which is created by dissolved gas entrapped  
179 in lava during scoria emission. The mineralogy of rocks, the proportion of  
180 dissolved gas and the temperature of scoria during volcanic eruption, all

181 affect upon the porosity and pore size distribution of pozzolan rocks.

182 Experimental data are less spread out for the water retention of bark  
183 compost. Contrary to pozzolan, the water retention measurements for bark  
184 compost are obtained on re molded and compacted samples. The porosity  
185 of compacted bark compost includes both the matric porosity of individual  
186 bark fragments and the structural porosity between bark fragments. As ob-  
187 served for natural soils (Dexter et al., 2008), water retention near saturation  
188 is linked to the structural porosity. We observe a very good linear rela-  
189 tionship between water retention data and apparent bulk density for matric  
190 potentials greater than  $-0.7$  m (data not shown). Variability in the water  
191 retention measurements is thus very low near saturation, since the apparent  
192 bulk density of bark compost samples is accurately controlled. For lower ma-  
193 tric potential values, the variability is due to the variability of matric porosity  
194 and pore size distribution of bark fragments. This experimental dispersion  
195 is relatively low, since the highest standard deviation value is  $0.02 \text{ m}^3/\text{m}^3$ .

196 Figs. 2 show that the van Genuchten model adequately fits water re-  
197 tention experimental data. The estimated uncertainty distributions have  
198 a similar behavior to those of the experimental ones: a lower level of un-  
199 certainty for compost than for pozzolan, particularly for matric potentials  
200 between  $-0.01$  m and  $-1$  m, and a higher level of uncertainty near satu-  
201 ration. For both materials, the most variable and least variable parameter,  
202 respectively, are  $h_e$  and the  $n$  exponent, with respective coefficient of varia-  
203 tions of approximately 20% and 1 % for bark compost data, and 35% and 1  
204 % for pozzolan aggregates data (see Table 1). The  $h_e$  parameter is a scale  
205 parameter, which is related to the entry point of air into the studied ma-

206 terial, whereas parameter  $n$  is a shape parameter related to the pore size  
 207 distribution (Kutilek and Nielsen, 1994): a greater scattering of parameter  
 208  $h_e$  could thus be linked to the macro porosity variability. A slight variability  
 209 in exponent  $n$  is representative of a homogeneous meso- and micro pore size  
 210 distribution for both materials.

### 211 2.3. Hydraulic conductivity curves and associated uncertainties

212 The Mualem-van Genuchten model (van Genuchten, 1980) is fitted to  
 213 the experimental data to obtain the hydraulic conductivity curve, i.e. the  
 214 relation between  $K(h, \mathbf{x}, t)$  [ $L.T^{-1}$ ], the hydraulic conductivity, and  $h(\mathbf{x}, t)$ ,  
 215 the matric water potential, as follows

$$K(h, \mathbf{x}, t) = K_{Sat} \cdot \Theta^{0.5}(h, \mathbf{x}, t) [1 - (1 - \Theta^{1/m})^m]^2 \quad (2)$$

216 where

$$\Theta(h, \mathbf{x}, t) = (\theta(h, \mathbf{x}, t) - \theta_r) / (\theta_s - \theta_r) = \left[ 1 + \left( \frac{h(\mathbf{x}, t)}{h_e} \right)^n \right]^{-m}. \quad (3)$$

217 The resulting uncertainty distributions of the hydraulic conductivity for  
 218 pozzolan and compost are presented in Figs. 3. The estimated values of the  
 219 Mualem-van Genuchten model parameters for compost and pozzolan and the  
 220 standard deviations of the associated uncertainty distributions are displayed  
 221 in Table 2.

222  $K_{Sat}$  experimental values range from  $10^{-7}$  to  $10^{-3}$  m.s $^{-1}$  for pozzolan  
 223 samples. The conductivities at saturation of “porous” blocks are higher than  
 224 those of “dense” blocks (not shown here). The relative standard deviation  
 225 of  $K_{Sat}$  is quite low for compost. This is expected as explained in the Ap-  
 226 pendix. For the unsaturated part of the hydraulic conductivity curve, the

227 scattering of  $(K, h)$  experimental data found for pozzolan and bark compost  
228 materials are similar to the scattering of data found for natural soils using  
229 the Wind evaporation method (Tamari et al., 1993). We observe a lack of  
230 experimental values between the data obtained under saturated and unsat-  
231 urated conditions. This is due to the limited accuracy of matric potential  
232 sensors and to the Wind evaporation method: it is necessary to have signifi-  
233 cant matric potential gradients between two successive sensors to compute an  
234 accurate value of the unsaturated hydraulic conductivity. This is usually not  
235 achieved close to saturation (Tamari et al., 1993). Despite this limitation,  
236 direct computation of  $K$  values can be obtained using the Wind evapora-  
237 tion. This is not the case for inverse methods used either in the one-step  
238 or the multi-step outflow methods (Hopmans et al., 2002), where only curve  
239 parameters are fitted.

240 Figs. 3 show that, as expected, the estimated uncertainty of the hydraulic  
241 conductivity of pozzolan is greater than that of bark compost. The uncer-  
242 tainty distribution of parameter  $n$  is very low for both materials (see Table  
243 2). For the  $h_e$  and  $K_{sat}$  parameters, the uncertainty is greater for pozzolan  
244 material than for bark compost material.

### 245 **3. Computation of effective hydraulic parameters and associated** 246 **uncertainties**

247 Effective hydraulic parameters are determined by simulating numerically  
248 a water flow, under specific conditions, in a three-dimensional representation  
249 of the heterogeneous material. This requires the preliminary solving of the  
250 highly non-linear Richards equation (RE). Simulations are performed herein

251 with a specific C++ parallelized code. The effective hydraulic properties  
 252 are then modeled by fitting parametric models on the simulated water re-  
 253 tention and conductivity values. The uncertainties on these properties are  
 254 estimated using the bootstrap method, as described in the previous section.  
 255 The followed procedure is summarized in Fig. 1, step 2.

### 256 3.1. C++ parallelized code and simulation configuration

257 The three-dimensional variably saturated flow modeling is based on the  
 258 non-linear Richards equation. The mixed form of RE obtained by combining  
 259 the mass conservation law with the generalized Darcy equation is

$$\frac{\partial \theta(h, \mathbf{x}, t)}{\partial t} = \nabla \cdot (K(h, \mathbf{x}, t) \nabla (h(\mathbf{x}, t) + z)) + Q(\mathbf{x}, t) \quad (4)$$

260 where  $z$  is the upward vertical coordinate and  $Q(\mathbf{x}, t)$  is a sink or/and source  
 261 term. Constitutive functions depending on the materials considered link  
 262  $h(\mathbf{x}, t)$ ,  $\theta(h, \mathbf{x}, t)$  and  $K(h, \mathbf{x}, t)$  and close (4). Various initial and boundary  
 263 conditions can complete the parabolic system of partial differential equations.

264 Water flow is solved using the mixed form of the Richards equation, for  
 265 which a perfect mass balance is ensured (Celia et al., 1990; Kavetski et al.,  
 266 2001; Renaud et al., 2003 to cite a few). Spatial discretization is performed  
 267 using the Galerkin-type linear isoparametric finite elements (Dhatt et al.,  
 268 1984; Ju and Kung, 1997). The modified Picard iteration scheme is imple-  
 269 mented in a fully implicit Euler time discretization. Different convergence  
 270 criterion can be used, as explained in Huang et al. (1996). An adaptive time  
 271 step adjustment is implemented to improve numerical efficiency (Kavetski et  
 272 al., 2001). Time and spatial discretizations result in the following system of

273 linear equations

$$\begin{aligned} & \left[ \frac{[M^{t+1,m}][C^{t+1,m}]}{\Delta t} + [K^{t+1,m}] \right] \{\delta_u^m\} = \\ & \{F^{t+1,m}\} - \frac{[M^{t+1,m}]}{\Delta t} \{\theta^{t+1,m}\} + \frac{[M^{t+1,m}]}{\Delta t} \{\theta^t\} - [K^{t+1,m}] \{u^{t+1,m}\} \end{aligned} \quad (5)$$

274 where  $t$  and  $m$  denote, respectively, time and inner iteration levels,  $u = h + z$   
275 and  $\delta_u^m = u^{t+1,m+1} - u^{t+1,m}$ ,  $[M]$  and  $[K]$  are the global mass and stiffness  
276 matrices,  $F$  includes the source/sink terms and  $[C(h, \mathbf{x}, t)]$  is the specific  
277 moisture capacity function matrix.

278 A C++ object oriented code has been developed to solve (5) and to deter-  
279 mine the water matric potential and the water flux at each node/boundary  
280 of the finite element mesh grid for an unsaturated medium. Our numer-  
281 ical results are found to corroborate analytical results published by Tracy  
282 (2007), Fityus and Smith (2001) or purely numerical results proposed by  
283 Vanderborght et al. (2005).

284 Due to the specific composition of the green roof substrate, very fine  
285 spatial grids are required, leading to huge CPU time and storage cost. This  
286 major drawback is overcome by a parallelization of the code (Hardelauf et al.,  
287 2007; Herbst et al., 2008). MPI (<http://www.mpi-forum.org/>) and PETSc  
288 (<http://www.mcs.anl.gov/petsc/>) libraries are used herein to parallelize the  
289 C++ sequential code.

290 Numerical simulations are performed on a typical soil core to compute  
291 the effective parameters at the Darcy scale. In our case, the green roof  
292 substrate is represented by a cylinder of the following dimensions: height =  
293 7 cm and diameter = 15 cm. This cylinder is discretized with 507553 nodes  
294 and 3216152 elements. The average length of each edge is approximately 1.5

295 mm. As mentioned in the Appendix, the pozzolan grain size distribution is  
296 the following: 2/3 of the pozzolan grain diameters ranged from 3 to 6 mm,  
297 and 1/3 from 7 to 15 mm. A specific algorithm is developed to model the  
298 geometry and distribution of pozzolan. This algorithm takes into account a  
299 mesh of the cylinder obtained by GMSH (<http://geuz.org/gmsh/>). Grains  
300 of pozzolan are then created by randomly selecting a seed represented by  
301 an element of the mesh. The volume of the grain is randomly chosen from  
302 the known grain diameter distribution and the pozzolan grains are assumed  
303 to be spheric. The grains are then iteratively built by randomly selecting  
304 and aggregating adjacent elements of the growing irregular seeds until the  
305 required grain volumes are reached. Fig. 4 shows a typical mesh used in the  
306 simulations.

### 307 *3.2. Method used to compute effective parameters*

308 The effective parameters are obtained using a steady-state flow simula-  
309 tion, as explained in Samouëlian et al. (2007) or Samouëlian et al. (2011).  
310 The interval under consideration is  $[-10^2, -10^{-2}]$  m, which corresponds to  
311 the validity range of the numerical code. The same water matric potential,  
312 a Dirichlet type condition, is applied to the upper and the lower boundaries  
313 of the cylinder. This leads to a constant water matric potential throughout  
314 the medium in the case of homogeneous materials. The vertical boundaries  
315 are impermeable. To obtain the hydraulic conductivity, the calculated wa-  
316 ter flux is divided by the surface of the upper boundary. In the case of a  
317 heterogeneous medium, the same configuration leads to an almost constant  
318 water matric potential in the medium, and the so-called effective hydraulic  
319 conductivity of the composite substrate is equal to the average water flux

320 density across the horizontal boundaries. The water retention is calculated  
321 for each element with a simple arithmetic average. These conductivity and  
322 water retention values are relative to the matric potential value set at the  
323 boundaries, even if local gradients of matric potential are present within the  
324 heterogeneous medium. The computation is thus repeated for several water  
325 matric potential values to plot the conductivity and retention curves.

326 To take into account uncertainties in the hydraulic properties of pozzolan  
327 and compost, the computation of the effective hydraulic conductivity and  
328 water retention for each water matric potential value is repeated for a sin-  
329 gle set of component properties randomly sampled from their uncertainty  
330 distributions. The spatial distribution of the pozzolan grains in the mesh  
331 is different for each repetition and is generated randomly as explained in  
332 section 3.1. The sampling of pozzolan and compost properties is performed  
333 independently for each water matric potential value.

334 The choice of the number and values of water matric potential points,  
335 and the number of replicates for each water matric potential value, directly  
336 affects the computational cost of the estimation of the effective properties  
337 and of their level of uncertainty. An optimal experimental design technique  
338 is used to guide these choices. A D-optimal criterion (Atkinson and Donev,  
339 1992) is computed to fit the Mualem-van Genuchten and the van Genuchten  
340 models. The aim is to minimize this D-criterion, which is the determinant of  
341 the error covariance matrices of the models parameters. Several contrasted  
342 water matric potential distributions of points are considered in the bounded  
343 interval  $[-10^2, -10^{-2}]$  m: regular distribution, log-regular distribution and  
344 quantiles of beta distributions to concentrate points on the left, the right

345 or the center of the interval. The log-regular distribution appears to be  
 346 the best compromise with respect to the criterion values computed for both  
 347 models for a number of water matric potential values. Then, an optimization  
 348 of the ratio between the number of water matric potential points and the  
 349 number of replicates, for a given computational cost corresponding to 200  
 350 simulations, is computed with this log-regular distribution. In the end, the  
 351 D-optimal design, among those tested, is a log-regular repartition of 4 water  
 352 matric potential points with 50 replicates. For the Mualem-van Genuchten  
 353 model fit, prior information from the Wiener bounds on  $K_{sat}$  is considered  
 354 to regularize the fitting problem due to the lack of data at  $h = 0$ .

355 *3.3. Effective water retention and hydraulic conductivity curves and associ-*  
 356 *ated uncertainties*

357 Various analytical bounds or estimations of effective hydraulic conductiv-  
 358 ities can be found in the literature (Matheron, 1967; Renard and de Marsily,  
 359 1997) . The Wiener bounds give a fundamental inequality which is always  
 360 valid. Let  $\mu_{a|K}$  and  $\mu_{h|K}$  be the arithmetic and harmonic means of conduc-  
 361 tivity values,  $\omega_C$  and  $\omega_P$  the volumetric proportion of each material, and  $K_C$   
 362 and  $K_P$  the hydraulic conductivities of compost and pozzolan, respectively.  
 363 For each water matric potential  $h$ , the effective conductivity  $K_{eff}$  can be  
 364 bounded as follows

$$\mu_{h|K} = \frac{1}{\omega_C/K_C + \omega_P/K_P} \leq K_{eff} \leq \mu_{a|K} = \omega_C K_C + \omega_P K_P.$$

365 Note that the Wiener bounds presuppose a plane layered structure of the  
 366 medium. The harmonic and arithmetic means are obtained, respectively,

367 when the water flux is perpendicular or parallel to the main orientation of  
368 the layered surface. For a statistically homogeneous and isotropic medium,  
369 Matheron (1967) proposes an estimation of the effective conductivity cal-  
370 culated by a geometric weighted average of the arithmetic and harmonic  
371 means  $\mu_{a|K}$  and  $\mu_{h|K}$ . This curve is defined by  $\mu_{M|K} = \mu_{a|K}^\alpha \mu_{h|K}^{1-\alpha}$ , where  
372  $\alpha = (D - 1)/D$  and  $D$  is the dimension of the problem.

373 Figs. 5 show the means and standard deviations of the 50 effective con-  
374 ductivity values at the 4 water matric potential values, as well as the means  
375 of the corresponding Wiener bounds and Matheron estimations. The means  
376 of the effective conductivity values, for each water matric potential value,  
377 must be included into the means of the corresponding Wiener bounds. The  
378 crosses which can be observed in Figs. 5 are well-bounded, validating the  
379 numerical procedure developed to determine the effective values. Note that  
380 the means of the effective conductivity values are closer to the arithmetic  
381 mean curve. They are above the Matheron mean curve before the intersec-  
382 tion between the Wiener curves, and below after that intersection. Fig. 6  
383 presents the means and standard deviations of the effective retention values.  
384 They are very close to the arithmetic mean curve. This result is already  
385 obtained by several authors (Samouëlian et al., 2007; Samouëlian et al., 2011  
386 ; Vogel et al., 2008 among others). Under quasi-static conditions and with-  
387 out dynamic effects, the water retention curve presents a capacitive property  
388 (Vogel et al., 2008) and the effective water retention curve can be calculated  
389 from the additive properties of the local water retention (Samouëlian et al.,  
390 2007). The standard deviations of the effective conductivity and retention  
391 values computed for the four water potential values are between those ob-

392 tained for bark compost and pozzolan, and close to the standard deviation  
393 of their arithmetic means (results not shown).

394 The uncertainty distributions of the effective water retention and the  
395 hydraulic conductivity are presented in Figs. 7. Estimated values and stan-  
396 dard deviations for the corresponding parameters of the van Genuchten and  
397 Mualem-van Genuchten models are displayed in Tables 1 and 2.

398 The estimated uncertainties for the effective parameters are relatively low  
399 and generally lower to those of bark compost and pozzolan under unsaturated  
400 conditions. This is mainly due to the size (number of replicates  $\times$  number of  
401 water potential values), and to a lower extent, given this size, to the optimal  
402 choice of the numerical experimental design used for computing the effective  
403 values. These uncertainties increase closer to saturation, following the same  
404 trend as the one observed for individual components. The standard devia-  
405 tions of most of the van Genuchten and Mualem-van Genuchten parameters  
406 estimated for the effective material are lower than the ones estimated for  
407 bark compost and pozzolan. The standard deviations of the parameters, di-  
408 rectly linked to saturated conditions ( $K_{Sat}$  and  $\theta_s$ ) estimated for the effective  
409 material, are between those estimated for bark compost and pozzolan.

410 To conclude this section, the methodology using an optimal sampling  
411 design leads to “well defined” effective properties. We show that the un-  
412 certainties of the effective properties are lower than the uncertainties of the  
413 properties of each material. The reduction in the level of uncertainty is more  
414 pronounced for the van Genuchten parameters associated to the dry part of  
415 the properties ( $\theta_r, h_e, n$ ) than for the ones associated to the wet part of the  
416 properties ( $\theta_s, K_{sat}$ ).

417 **4. Evaluation of the homogenization approach under dynamic evap-**  
418 **oration**

419 The reliability of the computed effective parameters is evaluated using  
420 simulations of dynamic scenarios. Our aim herein is to cross-check results  
421 obtained by simulating the evolution of water matric potential versus time  
422 with the effective medium and the heterogeneous material, for various points  
423 of the soil core described in section 3.1. The impacts of the uncertainties  
424 estimated for the hydraulic properties on the simulation results are also com-  
425 pared. The followed procedure is summarized in Fig. 1, step 3.

426 A time-variable flux of evaporation ranging from  $1.9 \text{ mm.d}^{-1}$  to  $0.9 \text{ mm.d}^{-1}$   
427 is applied to the top surface of the soil core at  $z = 0$ . The values of the time-  
428 variable flux are representative of usual experimental conditions when using  
429 the Wind evaporation method. The other boundaries are impermeable. The  
430 initial condition is that of a quasi-saturated medium with  $h(\mathbf{x}, t = 0) = -9.5$   
431 cm for all depths. For  $h = -100$  m, the flux type boundary conditions are  
432 switched to Dirichlet conditions. The simulations last 10 days to ensure a  
433 strong evaporation and a switch from flux to Dirichlet conditions at the upper  
434 part of the soil core.

435 200 simulations are performed for the bi material configuration and for the  
436 equivalent homogeneous material, by randomly sampling the corresponding  
437 hydraulic properties in their uncertainty distributions. For each simulation,  
438 4 sets of 5 points are considered to monitor the matric potential. They are  
439 taken for  $z = 0$  cm,  $z = -0.2$  cm,  $z = -1.1$  cm and  $z = -4.8$  cm. For  
440 each depth, the arithmetic mean values of matric potential are computed  
441 on the 5 points. The distribution of these mean values obtained for the bi

442 material configuration are then compared to the distribution obtained for the  
443 equivalent homogeneous configuration at each depth.

444 Three snapshots of water potential values obtained during the evapo-  
445 ration process are presented in Figs. 8 for the bi material configuration.  
446 Heterogeneous spatial distributions of these values are observed at the upper  
447 surface of the soil core at  $t = 2$  days and  $t = 6$  days. Blue shades represent  
448 the gradients due to the geometrical distribution of the two materials. Con-  
449 sequently, isovalues of  $h$  do not correspond to horizontal planes. At  $t = 10$   
450 days, the Dirichlet condition replaces the flux condition at the upper surface,  
451 which leads to a uniform spatial distribution of water matric potential values  
452 at  $z = 0$ . A gradually stronger vertical gradient could be seen in-depth as  
453 evaporation takes place.

454 Figs. 9 present the uncertainty distributions of water matric potential  
455 mean values per depth for the bi material configuration and the corresponding  
456 effective homogeneous material configuration. The uncertainty distributions  
457 obtained for the effective homogeneous material configuration are clearly  
458 less scattered than those obtained for the bi material configuration, and are  
459 included in their [25th, 75th] percentile ranges (not shown here). This is a  
460 direct consequence of the lower level of uncertainties of the effective hydraulic  
461 properties compared to those of compost and pozzolan.

462 The means of these uncertainty distributions for each simulation config-  
463 uration and depth are also presented in Figs. 9. The curves obtained for the  
464 effective homogeneous material and the explicit two-component medium are  
465 similar. This confirms the validity of our approach. However, some discrep-  
466 ancies appear as simulation time increases. Table 3 shows the mean water

467 matric potential values and the mean water content values for both configu-  
468 rations at  $t_{max} = 10$  days, the final time point of the evaporation simulation.  
469 Relative differences between the two configurations are quite high for water  
470 matric potentials, and are more pronounced in-depth. However, these rela-  
471 tive differences concern an area of the core where the porous media are dry.  
472 Water content values of both the bi material and the homogeneous material  
473 configurations are computed from these water matric potentials using the  
474 van-Genuchten model and the parameters estimated for the effective mate-  
475 rial configuration given in Table 1. These water content values presented  
476 in Table 3 show only slight differences between the two configurations, and  
477 the relative differences (between 2.1% and 6.4% at 10 days) are lower than  
478 those of the water matric potentials. Note that these discrepancies may be  
479 due to the non-equilibrium flow process, a consequence of the occurrence  
480 of transient processes during the dynamic simulation. This time-dependent  
481 phenomenon is not accounted for during the homogenization process since  
482 the determination of the effective properties is performed under successive  
483 states of equilibrium.

## 484 **5. Conclusion**

485 The hydraulic properties of a heterogeneous medium are studied at the  
486 Darcy scale using two different approaches. The first methodological ap-  
487 proach consists in determining the water retention and hydraulic conductiv-  
488 ity curves for the components of the heterogeneous medium. The material  
489 considered here is a green roof substrate, which is a composite of compressible  
490 materials, bark compost, and of aggregates of volcanic rock, pozzolan. As-

491 sociated uncertainties are evaluated using a bootstrap method. It is shown,  
492 on a virtual evaporation experiment, that the impact of these uncertainties  
493 on the simulated water matric potential is high.

494 The second approach consists in considering the heterogeneous medium  
495 as an homogeneous material. Effective water retention and hydraulic conduc-  
496 tivity curves are fitted on values computed for several water matric potentials  
497 using numerical steady-state scenarios on the heterogeneous material. As-  
498 sociated uncertainties of these properties are also evaluated, considering the  
499 uncertainties of the hydraulic properties of each component. To that effect,  
500 for each hydraulic property,  $N$  couples of curves are sampled in the uncer-  
501 tainty distributions of the components in an independent way for a set of  
502 water matric potential values.  $N$  is set at a high value, and the water ma-  
503 tric potential values are optimally chosen. We show that this methodology  
504 leads to very low levels of uncertainties in the effective properties of the ma-  
505 terial. A direct consequence of this approach is that the uncertainties of  
506 simulated water potential for the effective material are very low compared  
507 to those obtained on the heterogeneous medium. This shows that the use of  
508 effective properties for a heterogeneous material reduces the impact of the  
509 uncertainties in the properties of its components. This is of importance since  
510 the uncertainties linked to the experimental disposal and to the variability of  
511 the materials properties may be high, as shown in the first part of the study.  
512 Note that the level of uncertainty obtained here for the simulation of water  
513 matric potential in the effective material under evaporation conditions might  
514 not be representative of the level of uncertainty expected on the simulation of  
515 a real evaporation experiment. In this last case, other types of uncertainties,

516 such as uncertainties on initial and boundary conditions for example, must  
517 be taken into account.

518 Although the level of uncertainties obtained on the simulations of the  
519 water matric potential differs for the heterogeneous and effective materials,  
520 their mean values are almost similar. This confirms the adequacy of the  
521 strategy developed herein. The slight discrepancies observed between these  
522 means may be due to the absence of non-equilibrium term in the simulation  
523 model used. This term could be included in the scope of future studies.

## 524 **Acknowledgment**

525 This work was supported by the French National Research Agency (ANR)  
526 through the “Habitat intelligent et solaire photovoltaïque” program (project  
527 AGROBAT ANR-09-HABISOL-001). We also thank the CINES (Centre  
528 Informatique National de l’Enseignement Supérieur, France) for offering us  
529 access to the supercomputer JADE to conduct these calculations successfully.  
530 The authors wish to thank Profs. L. Di Pietro, G. Micolau, H. Bolvin and Dr.  
531 C. Doussan for their helpful comments and careful readings of the manuscript.

532 **Appendix: experimental procedures**

533 The green roof substrate under study is composed of a combination of 40%  
534 organic material (bark compost) and 60% volcanic material (pozzolan). This  
535 combination corresponds to the volumetric proportions which are actually  
536 used in in situ environments.

537 *Determination of solid density and apparent bulk density of compost and*  
538 *pozzolan*

539 Pozzolan materials are extracted in a quarry located in the “Massif Cen-  
540 tral” mountain, in the center of France. Chemical composition of pozzolan is  
541 given by the operator of the quarry ( $\text{SiO}_2$  : 42–55%;  $\text{Al}_2\text{O}_3$  : 12–24%;  $\text{Fe}_2\text{O}_3$  :  
542 8 – 20%). The pozzolan grain size distribution is the following: 2/3 of the  
543 pozzolan grain diameters ranged from 3 to 6 mm, and 1/3 from 7 to 15 mm.  
544 Bark compost is provided by an industrial partner and the precise composi-  
545 tion of this compost is confidential.

546 The properties of the two materials are measured on samples of both  
547 materials, and are measured at the same bulk density [ $M.L^{-3}$ ] as they occur  
548 in the actual substrate.

549 Samples are crunched, sieved at 315  $\mu\text{m}$  and air dried in the oven for 24 h  
550 at 105 °C. Solid particles are then placed in the measurement chamber of a He  
551 pycnometer and solid bulk density is determined using the Boyle law (Dane  
552 and Hopmans, 2002). The apparent bulk density of pozzolan aggregates  
553 is measured on replicates with diameters varying from 7 to 15 mm, using  
554 Archimede’s law and buoyancy measurements in water. The aggregates are  
555 previously saturated in water for 24 h (Monnier et al., 1973). The apparent

556 bulk density of the composite substrate is measured using the core method  
557 (Dane and Hopmans, 2002) adapted for compacted and re molded samples.

558 Since bark compost is a compressible material, contrary to pozzolan, we  
559 follow the procedure described hereafter to be sure that the density of pure  
560 bark compost samples is the same as the density of bark compost present in  
561 the actual composite substrate: the complex substrate is characterized fol-  
562 lowing a standard compaction methodology, namely the Proctor compaction  
563 test, standard DIN 18127. The sample is struck 6 times by a 4.5 kg Proctor  
564 hammer from a height of 45 cm to obtain adequate compaction. The com-  
565 pacted sample obtained following this methodology is supposed to be repre-  
566 sentative of the in situ industrial execution of the green roofs (Forschungs-  
567 gesellschaft Landschaftsentwicklung Landschaftsbau e. V. - FLL, 2002). By  
568 knowing, on the one hand, the apparent bulk density of the substrate and  
569 of the pozzolan aggregates and, on the other hand, the solid density of bark  
570 compost and of pozzolan, we extrapolate the apparent bulk density of bark  
571 compost in the actual composite substrate.

572 All of the measured properties are displayed in Table 4.

### 573 *Determination of water retention and associated uncertainties*

574 Water retention measurements are obtained using the suction table for  
575 small suctions (0.05, 0.54, 1.03, 2.01, 3.97, 6.91 kPa) and the pressure plate  
576 extractors for large suctions (10, 30, 50, 100, 300, 500 and 1500 kPa) (Dane  
577 and Hopmans, 2002). The total number of replicates differs for pozzolan and  
578 bark compost materials.

- 579 1. Since pozzolan aggregates are a natural material with a high level of  
580 variability due to geological variations occurring during their formation,

581 a large number of replicates are required to counter the effects of this  
582 natural heterogeneity. 10 different aggregates are used for each suction  
583 point. The aggregates taken for apparent bulk density measurements  
584 are also used for the 0 kPa suction point. Water saturated aggregates  
585 are gently placed onto a fine layer of kaolinite paste to ensure a good  
586 contact between aggregate pores and the sand layer (for suction tables)  
587 or the porous plate (for pressure plate extractors). A set time for sample  
588 equilibration of 3 days is respected.

589 2. Bark compost samples are compacted in the laboratory following a  
590 standard procedure to obtain a predetermined density of compost into  
591 the composite substrate, the variability of which is very low (see Table  
592 4). A low number of replicates are, therefore, required. 5 different bark  
593 compost samples are used for each suction point. To account for any  
594 natural variability in the density of bark compost within the compos-  
595 ite substrate, samples are compacted in small cylinders ranging from  
596 0.184 and 0.213 g.cm<sup>-3</sup>. Mean bulk density is 0.200 g.cm<sup>-3</sup>, which  
597 differs slightly from the theoretical bulk density of compost within the  
598 composite substrate (0.195 g.cm<sup>-3</sup>), due probably to experimental ap-  
599 proximations. After initial saturation, samples are placed onto the  
600 suction table or porous plate. Kaolinite paste is also used to increase  
601 the quality of the capillary connectivity between the sample and the  
602 sand layer or porous plate. The time needed for sample equilibrium is  
603 over one week for each suction point and is controlled by monitoring  
604 the water flow out of the pressure chamber.

605 *Determination of hydraulic conductivity and associated uncertainties*

606 Hydraulic conductivity is measured for pozzolan and bark compost un-  
607 der water-saturated and unsaturated conditions using two different meth-  
608 ods. Hydraulic conductivity at saturation  $K_{Sat}$  [ $L.T^{-1}$ ] is measured using  
609 a constant head permeameter (Chossat, 2005) for pozzolan cores and bark  
610 compost samples. Unsaturated hydraulic conductivity is measured using the  
611 Wind evaporation method (Tamari et al., 1993). Samples used for determin-  
612 ing the hydraulic conductivity at saturation are also used to determine the  
613 unsaturated hydraulic conductivities. As is the case of the water retention  
614 curve, the number of replicates differs for pozzolan and bark compost, and  
615 are adapted to the different variability of both materials: 10 replicates are  
616 used for pozzolan and 1 replicate is used for bark compost.

617 Samples of pozzolan are extracted from large blocks (volume of approxi-  
618 mately  $1 \text{ dm}^{-3}$ ). A classification of these blocks is initially made based on the  
619 visible porosity and the estimated bulk density: an equal number of “com-  
620 pact” and “porous” blocks in equal quantities are identified. 10 replicates  
621 are then cored from both types of blocks. The vertical walls of the clods are  
622 surrounded by heat shrink tubing to avoid preferential water flow along the  
623 walls during measurements. The uncertainty distribution of the measured  
624 hydraulic conductivity at saturation used in section 2.3 is estimated as the  
625 experimental variability of  $K_{Sat}$  measurements.

Samples of bark compost are obtained after their compaction up to  $0.195 \text{ g.cm}^{-3}$  in cylinders. A single replicate is used, since a low experimental variability is expected as the compaction procedure is accurately performed and leads to a very low level of variability in the porosity obtained (see

Table 4). Porosity  $\phi$  of bark compost is measured for this single sample. The uncertainty of the measured saturated hydraulic conductivity could thus be estimated from the variability in the porosity values using the Kozeny-Carman model (Kutilek and Nielsen, 1994). A simple error propagation computed using this model, assuming a log-normal distribution of  $K_{Sat}$ , gives rise to

$$\text{var} [\log(K_{Sat})] = \left( \frac{3 - \phi}{\phi(1 - \phi)} \right)^2 \text{var}(\phi).$$

626 For measuring the unsaturated hydraulic conductivity, pozzolan clods and  
 627 bark compost are equipped with sufficient microtensiometers to obtain an  
 628 accurate estimation of their hydraulic properties (Tamari et al., 1993). After  
 629 the sample saturation, water is allowed to evaporate from the upper surface  
 630 of each core under laboratory conditions, i.e. conditioned atmosphere at 24  
 631 °C under atmospheric pressure. The base of each core is sealed to prevent  
 632 downward flux.

- 633 Atkinson, A.C., Donev, A.N., 1992. Optimum Experimental Designs, vol-  
634 ume 8 of Oxford Statistical Science Series, 1st edn. Oxford University Press,  
635 Oxford, UK, 352pp.
- 636 Celia, M.A., Bouloutas, E.T., Zarba, R.L., 1990. A general mass-  
637 conservative numerical solution for the unsaturated flow equation. *Water*  
638 *Resour. Res.* 26(7), 1483–1496.
- 639 Chossat, J.C., 2005. La mesure de la conductivité hydraulique dans les sols  
640 - Choix des méthodes, 1st edn. Tec et Doc - Lavoisier Editions, London,  
641 Paris, New York, 720pp.
- 642 Christiaens, K., Feyen, J., 2001. Analysis of uncertainties associated with  
643 different methods to determine soil hydraulic properties and their propaga-  
644 tion in the distributed hydrological MIKE SHE model. *J. Hydrol.* 246(1-4),  
645 63–81.
- 646 Coleman, T.F., Li, Y., 1996. An Interior, Trust Region Approach for Non-  
647 linear Minimization Subject to Bounds. *SIAM J. Optimiz.* 6(2), 418–445.
- 648 Coppola, A., Basile, A., Comegna, A., Lamaddalena, N., 2009. Monte Carlo  
649 analysis of field water flow comparing uni- and bimodal effective hydraulic  
650 parameters for structured soil. *J. Contam. Hydrol.* 104(1-4), 153–165.
- 651 Dane, J.H., Hopmans, J.W., 2002. Methods of soil analysis: Part 4 Physical  
652 methods, In: Dane, J.H., Topp, G.C. and Campbell, G.S. (Ed.) *Soil Science*  
653 *Society of America, Madison:SSSA book series 5*, 1662pp.
- 654 Danquigny, C., Ackerer, P., 2005. Experimental determination of equivalent

655 parameters of a heterogeneous porous medium under uniform or radial flow.  
656 C. R. Geoscience. 337(6), 563–570.

657 Dexter, A.R., Czyz, E.A., Richard, G., Reszkowska, A., 2008. A user-  
658 friendly water retention function that takes account of the textural and  
659 structural pore spaces in soil. Geoderma. 143(3-4), 243–253.

660 Dhatt, G., Touzot, G., Lefrancois, E., 2007. Méthode des éléments finis, 4th  
661 edn. Hermes Science Publications - Lavoisier Editions, London, Paris, New  
662 York, 601pp.

663 Efron, B., Tibshirani, R., 1994. An Introduction to the Bootstrap, Mono-  
664 graphs on Statistics & Applied Probability (Book 57), 1st edn. Chapman  
665 & Hall/CRC, London, UK, 456pp.

666 Fityus, S.G., Smith, D.W., 2001. Solution of the unsaturated soil mois-  
667 ture equation using repeated transforms. Int. J. Numer. Anal. Methods  
668 Geomech. 25(15), 1501–1524.

669 Forschungsgesellschaft Landschaftsentwicklung Landschaftsbau e.V.–FLL,  
670 2002. Guidelines for the planning, execution and upkeep of green-roof  
671 sites, 1st edn. Forschungsgesellschaft Landschaftsentwicklung Landschafts-  
672 bau e. V. - FLL, Bonn, Germany, 97 pp. URL: <http://www.fll.de>

673 Hardelauf, H., Javaux, M., Herbst, M., Gottschalk, S., Kasteel, R., Van-  
674 derborght, J., Vereecken, H., 2007. PARSWMS: A parallelized model for  
675 simulating three-dimensional water flow and solute transport in variably  
676 saturated soils. Vadose Zone J. 6(2), 255–259.

- 677 Herbst, M., Gottschalk, S., Reissel, M., Hardelauf, H., Kasteel, R., Javaux,  
678 M., Vanderborght, J., Vereecken, H., 2008. On preconditioning for a parallel  
679 solution of the Richards equation. *Comput. & Geosci.* 34(12), 1958–1963.
- 680 Hopmans, J.W., Šimůnek, J., Romane, N., Durner, W., 2002. Methods of  
681 Soil analysis - Part 4 Physical Methods, In: Dane, J.H., Topp, G.C. and  
682 Campbell, G.S. (Ed.) *Soil Science Society of America, Madison:SSSA book*  
683 *series 5, 1662pp.*
- 684 Huang, K., Mohanty, B.P., van Genuchten, Mth., 1996. A new convergence  
685 criterion for the modified Picard iteration method to solve the variably  
686 saturated flow equation. *J. Hydrol.* 178(1-4), 69–91.
- 687 Javaux, M., Vanclooster, M., 2006. Three-dimensional structure character-  
688 isation and transient flow modelling of a variably saturated heterogeneous  
689 monolith. *J. Hydrol.* 327(3-4), 516–524.
- 690 Ju, S.H., Kung, K.J.S., 1997. Mass types, element orders and solution  
691 schemes for the Richards equation. *Comput. & Geosci.* 23(2) 175–187.
- 692 Kavetski, D., Binning, P., Sloan, S.W., 2001. Adaptive time stepping and  
693 error control in a mass conservative numerical solution of the mixed form  
694 of Richards equation. *Adv. Water Resour.* 24(6), 595–605.
- 695 Kutilek, M., Nielsen, D.R., 1994. *Soil Hydrology*, 1st edn. Catena Verlag  
696 GMBH, Reiskirchen, Germany, 370pp.
- 697 Ma, D., Shao, M., Zhang, J., Wang, Q., 2010. Validation of an analytical  
698 method for determining soil hydraulic properties of stony soils using  
699 experimental data. *Geoderma.* 159, 262–269.

- 700 Manly, B.F.J., 2006. Randomization, Bootstrap and Monte Carlo Methods  
701 in Biology, 3rd edn. Chapman & Hall/CRC, London, UK, 480pp.
- 702 Matheron G., 1967. Eléments pour une Théorie des Milieux Poreux, 1st  
703 edn. Masson et Cie, Paris, France, 168pp.
- 704 Mohrath, D., Bruckler, L., Bertuzzi, P., Gaudu, J.C., Bourlet, M., 1997.  
705 Error analysis of an evaporation method for determining hydrodynamic  
706 properties in unsaturated soil. Soil Sci. Soc. Am. J. 61(3), 725–735.
- 707 Monnier, G., Stengel, P., Fiès, J.C., 1973. Une méthode de mesure de la  
708 densité apparente de petits agglomérats terreux. Application à l’analyse des  
709 systèmes de porosité du sol. Ann. agron. 24(5), pp. 533-545.
- 710 Pan, F., Ye, M., Zhu, J., Wu, Y.S., Hu, B.X., Yu, Z., 2009. Numerical eval-  
711 uation of uncertainty in water retention parameters and effect on predictive  
712 uncertainty. Vadose Zone J. 8(1), 158–166.
- 713 Peters, A., Durner, W., 2008. Simplified evaporation method for determin-  
714 ing soil hydraulic properties. J. Hydrol. 356(1-2), 147–162.
- 715 Renard, Ph., de Marsily, G., 1997. Calculating equivalent permeability: a  
716 review. Adv. Water Resour. 20(5-6), 253–278.
- 717 Renaud, J., Cloke, H., Wang, Y., Anderson, M., Wilkinson, P., Lloyd, D.,  
718 2003. Simulation numérique d’écoulements en milieu poreux avec l’équation  
719 de Richards. Eur. J. Comput. Mech. 12(2-3), 203–220.
- 720 Samouëlian, A., Vogel, H.J., Ippisch, O., 2007. Upscaling hydraulic conduc-

- 721 tivity based on the topology of the sub-scale structure. *Adv. Water Resour.*  
722 30(5), 1179–1189.
- 723 Samouëlian, A., Cousin, I., Dagès, C., Frison, A., Richard, G., 2011. De-  
724 termining the effective hydraulic properties of a highly heterogeneous soil  
725 horizon. *Vadose Zone J.* 10(1), 450–458.
- 726 Tamari, S., Bruckler, L., Halbertsma, J., Chadoeuf, J., 1993. A simple  
727 method for determining soil hydraulic properties in the laboratory. *Soil Sci.*  
728 *Soc. Am. J.* 57(3), 642–651.
- 729 Tracy, F.T., 2007. Three-dimensional analytical solutions of Richards' equa-  
730 tion for a box-shaped soil sample with piecewise-constant head boundary  
731 conditions on the top. *J. Hydrol.* 336(3-4), 391–400.
- 732 Vanderborght, J., Kasteel, R., Herbst, M., Javaux, M., Thiéry, D., Van-  
733 clooster, M., Mouvet, C., Vereecken, H., 2005. A set of analytical bench-  
734 marks to test numerical models of flow and transport in soils. *Vadose Zone*  
735 *J.* 4(1), 206–221.
- 736 van Genuchten, MTh., 1980. A closed-form equation for predicting the hy-  
737 draulic conductivity of unsaturated soils. *Soil Sci. Soc. Am. J.* 44(5), 892–  
738 898.
- 739 Vereecken, H., Kasteel, R., Vanderborght, J., Harter, T., 2007. Upscaling  
740 hydraulic properties and soil water flow processes in heterogeneous soils: a  
741 review. *Vadose Zone J.* 6, 1–28.
- 742 Vogel, H.J., Roth, K., 1998. A new approach for determining soil hydraulic  
743 functions. *Eur. J. Soil Sci.* 49(4), 547–556.

744 Vogel, H.J., Samouëlian, A., Ippisch, O., 2008. Multi-step and two-step  
745 experiments in heterogeneous porous media to evaluate the relevance of  
746 dynamic effects. *Adv. Water Resour.* 31(1), 181–188.

747 Vogel, H.J., Weller, U., Ippisch, O., 2010. Non-equilibrium in soil hydraulic  
748 modelling. *J. Hydrol.* 393(1-2), 20–28.

		$\theta_r$	$\theta_s$	$h_e$	$n$
Compost	Estimat. value	$8.66e^{-2}$	$5.55e^{-1}$	$7.47e^{-3}$	1.22
	$\sigma$	$5.92e^{-3}$ (6.9%)	$1.27e^{-2}$ (2.3%)	$1.63e^{-3}$ (21.8%)	$1.01e^{-2}$ (0.8%)
Pozzolan	Estimat. value	0( <i>fixed</i> )	$3.53e^{-1}$	$5.88e^{-3}$	1.29
	$\sigma$	0( <i>fixed</i> )	$1.63e^{-2}$ (4.6%)	$2.05e^{-3}$ (34.9%)	$1.11e^{-2}$ (0.9%)
Effective material	Estimat. value	$3.81e^{-2}$	$4.35e^{-1}$	$6.71e^{-3}$	1.26
	$\sigma$	$7.17e^{-4}$ (1.9%)	$1.36e^{-2}$ (3.1%)	$1.04e^{-3}$ (15.5%)	$2.74e^{-3}$ (0.2%)

Table 1: Estimated values and associated uncertainties of the van Genuchten model parameters for water retention of compost, pozzolan and effective material.

		$K_{Sat}$	$h_e$	$n$
Compost	Estimat. value	$3.04e^{-3}$	$9.72e^{-3}$	1.12
	$\sigma$	$1.03e^{-4}$ (3.4%)	$2.79e^{-4}$ (2.9%)	$8.87e^{-3}$ (0.8%)
Pozzolan	Estimat. value	$6.94e^{-6}$	$6.01e^{-1}$	1.02
	$\sigma$	$7.95e^{-6}$ (114.6%)	$9.90e^{-1}$ (164.7%)	$9.64e^{-3}$ (0.9%)
Effective material	Estimat. value	$9.36e^{-4}$	$2.28e^{-2}$	1.05
	$\sigma$	$8.91e^{-5}$ (9.5%)	$8.01e^{-4}$ (3.5%)	$1.91e^{-3}$ (0.2%)

Table 2: Estimated values and associated uncertainties of the Mualem-van Genuchten model parameters for hydraulic conductivity of compost, pozzolan and effective material.

		Depth= -0.2 cm	Depth= -1.1 cm	Depth= -4.8 cm
Water matric potential means	Effective homo- geneous material configuration	-45.78	-15.33	-5.68
	Bimaterial configura- tion	-53.71	-21.47	-8.36
	Relative differences	14.8%	28.6%	32.1%
Water content means	Effective homo- geneous material configuration	7.81 e-2	9.12 e-2	10.69 e-2
	Bimaterial configura- tion	7.65 e-2	8.68 e-2	10.00 e-2
	Relative differences	2.1%	4.9%	6.4%

Table 3: Means of all water matric potential and water content values for several depth and for the bi material and effective material configurations.

		Pozzolan aggregate	Complex substrate	Bark compost
Particle density	Mean	3.000	-	1.670
	$\sigma$ coefficient of variation	0.020 0.7%	- -	0.040 2.4%
Apparent bulk density	Mean	1.520	0.822	0.195
	$\sigma$ coefficient of variation	0.230 15.1%	0.002 0.2%	0.003 1.5%

Table 4: Mean and standard deviation values of the particle and apparent bulk densities for bark compost, pozzolan aggregate and complex substrate.

**List of captions**

Figure 1:

General flowchart of the approach. # is used to symbolise several samples or values. Blue color is used for the description of the processing of the heterogeneous material and its individual components, green color for the effective material, red color for the treatment of uncertainties.

Figure 2:

Uncertainty distributions of a) pozzolan and b) compost water retention values. Crosses and error bars represent means and  $\pm 1$  standard deviations of measured data and curves represent 0.5, 2.5, 25, 75, 97.5, 99.5 percentiles and median of the estimated water retention uncertainty distributions. Vertical axes are in log scale.

Figure 3:

Uncertainty distributions of a) pozzolan and b) compost hydraulic conductivity values. Crosses represent measured data and curves represent 0.5, 2.5, 25, 75, 97.5, 99.5 percentiles and median of the estimated hydraulic conductivity distributions. Data obtained for pozzolan samples are represented with the same symbol since experimental scattering largely overlaps from one sample to the other. Vertical and horizontal axes are in log scale.

Figure 4:

Typical heterogeneous mesh for the bi material configuration. Black or white zones correspond, respectively, to the pozzolan or bark compost components.

Figure 5:

Effective conductivity values computed from 200 compost and pozzolan properties for 4 water matric potential values. Crosses represent the mean and  $\pm 1$  standard deviations of the 50 computed values per water matric potential point, dotted lines are the means of the Wiener bounds and the plain line is the Matheron curve obtained from these mean curves. Fig. b) is an enhanced view of Fig. a). Vertical and horizontal axes are in log scale.

Figure 6:

Effective retention values computed from 200 compost and pozzolan properties for 4 water matric potential values. Crosses represent the mean and  $\pm 1$  standard deviations of the 50 computed values per water matric potential point and the plain line is the mean of the arithmetic mean curves obtained from the compost and pozzolan retention curves used. The horizontal axis is in log scale.

Figure 7:

Uncertainty distributions of a) effective hydraulic conductivity and b) water retention. Crosses and error bars represent means and  $\pm 1$  standard deviations of simulated data and curves represent 0.5, 2.5, 25, 75, 97.5, 99.5 percentiles and median of the estimated hydraulic conductivity and water retention distributions. The vertical axes are in log scale. The horizontal axis of plot a) is also in log scale.

Figure 8:

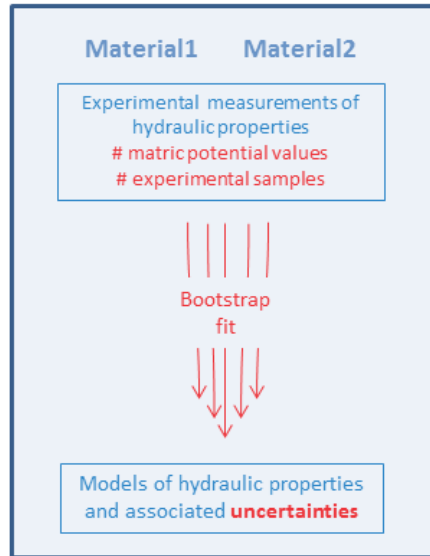
Snapshots of the evolution of the water potential according to time, at a)  $t = 2$  days, b)  $t = 6$  days and c)  $t = 10$  days. Scales for water matric potential are different for each snapshot.

Figure 9:

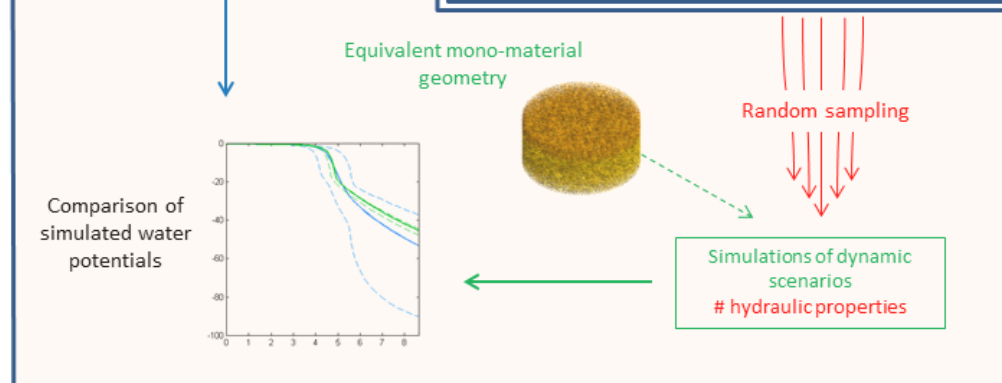
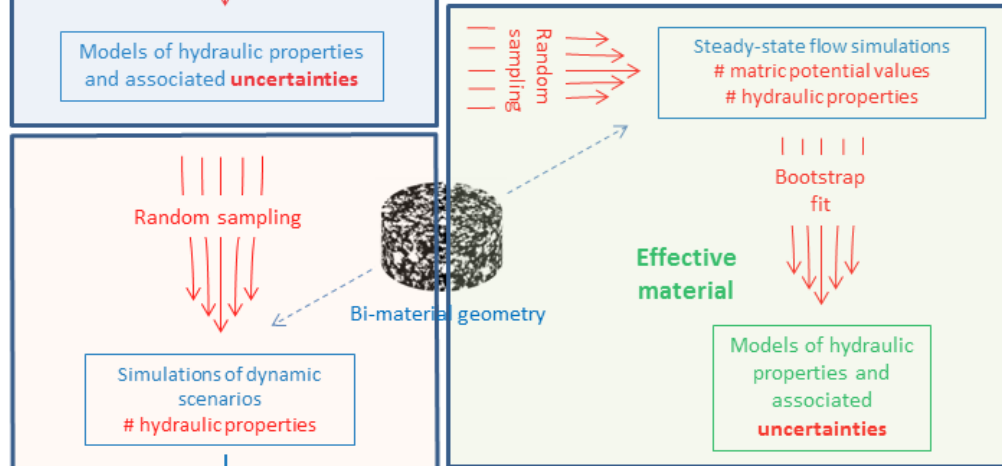
Uncertainty distributions of water matric potential values obtained by simulating evaporation using the heterogeneous green roof substrate (black curves) and using the corresponding computed effective homogeneous material (red curves). Dotted or solid curves represent, respectively, 0.5, 99.5 percentile or median values for the water matric potential distributions. The 4 graphs correspond to 4 various depths of the core.

Figure 1

Step1: Estimation of individual material properties

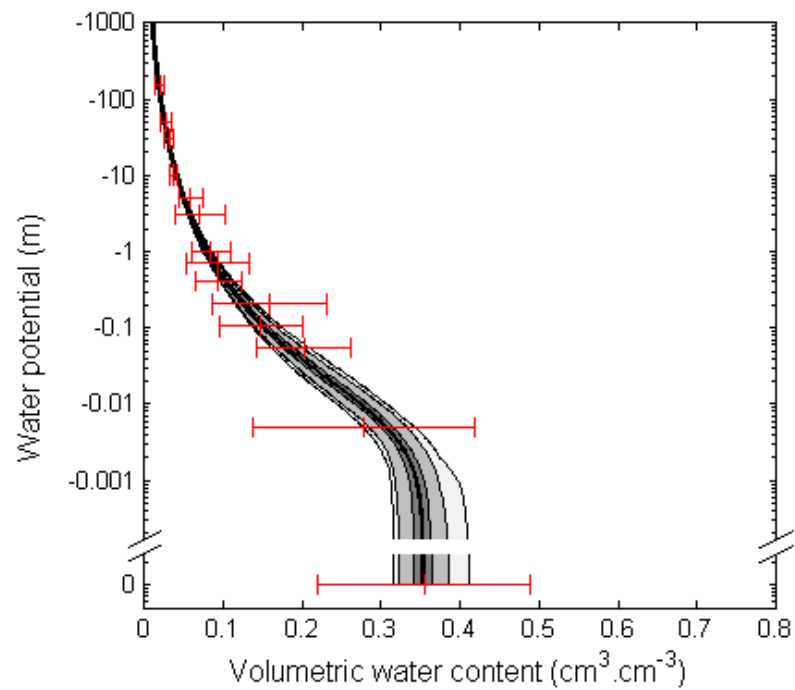


Step2: Computation of effective properties

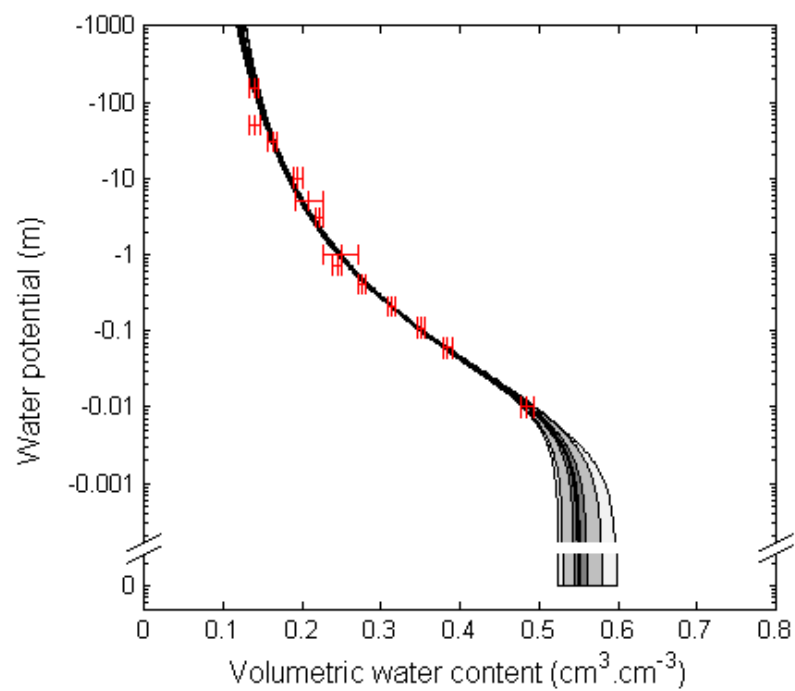


Step3: Evaluation of the homogenisation approach

Figure 2

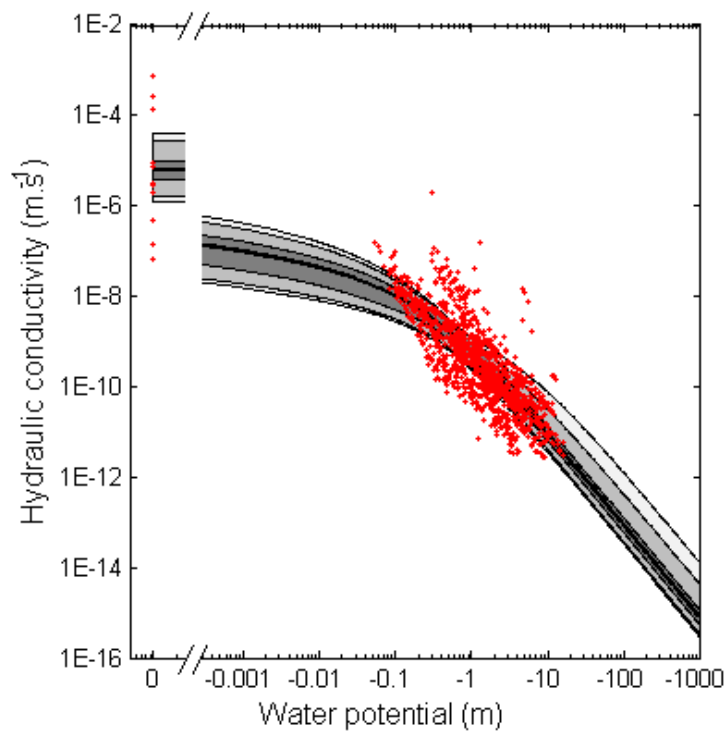


(a)

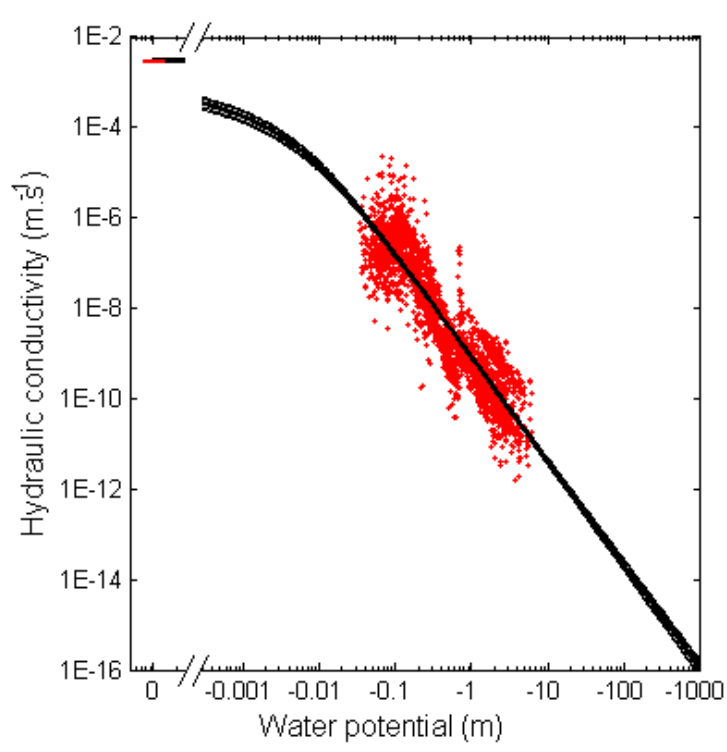


(b)

Figure 3



(a)



(b)

Figure 4

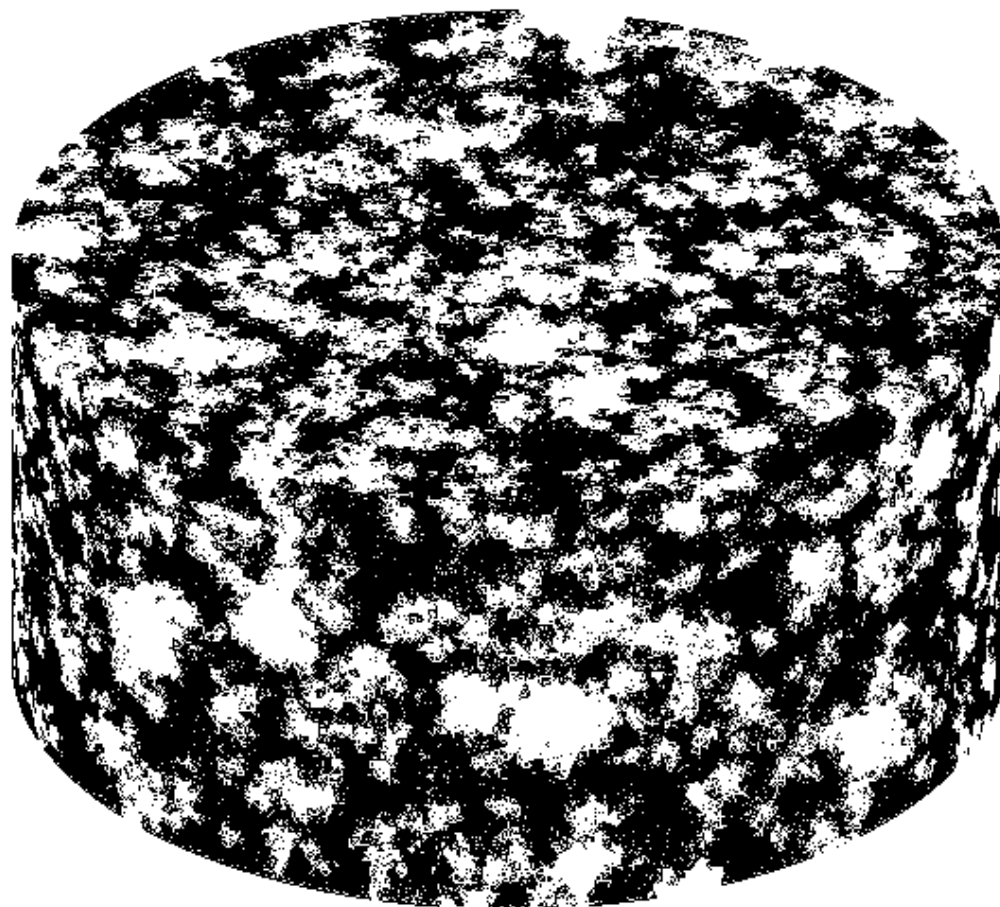
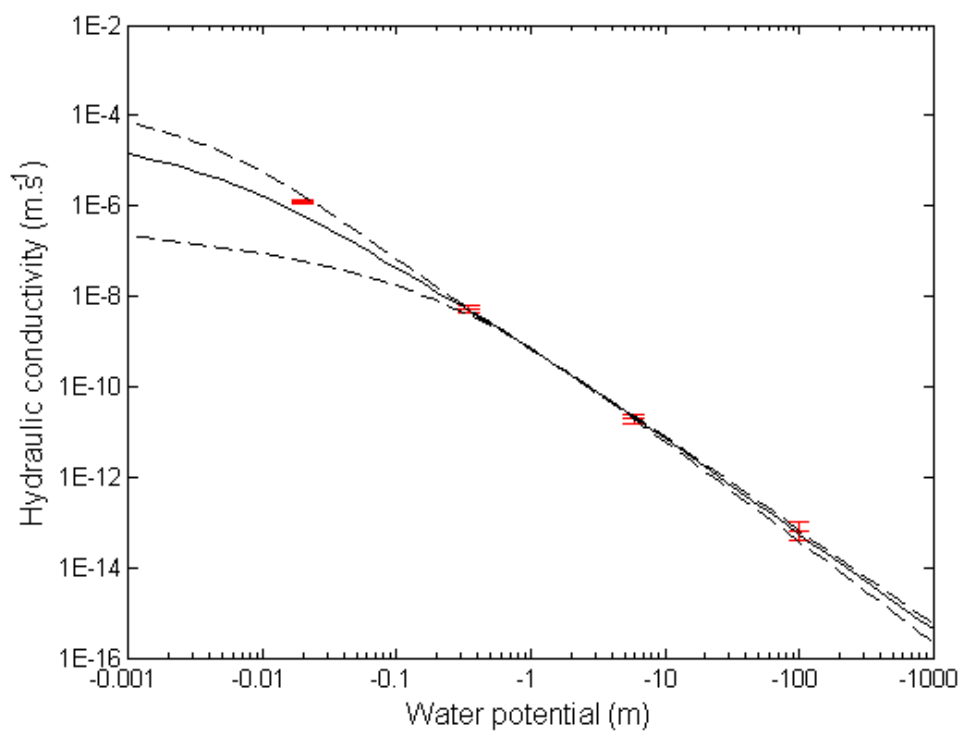
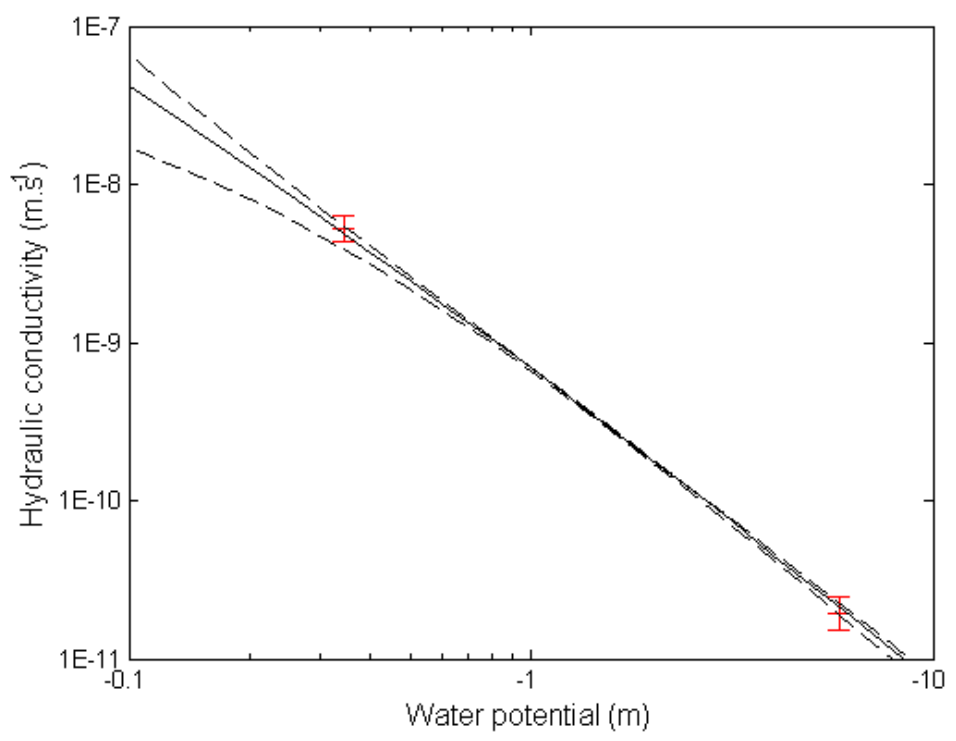


Figure 5



(a)



(b)

Figure 6

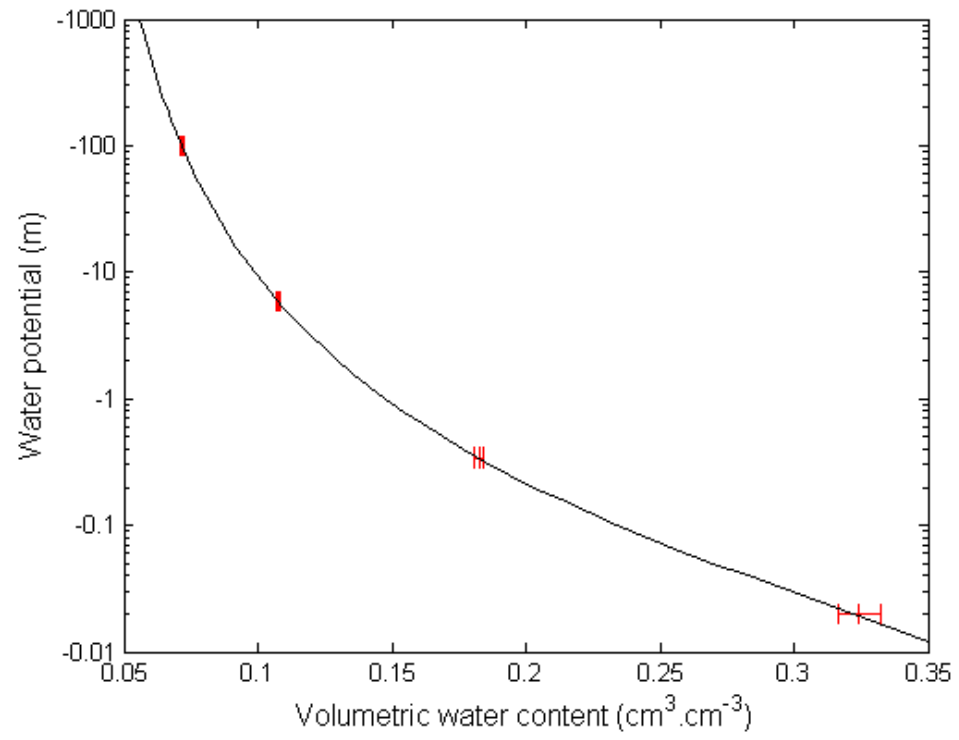
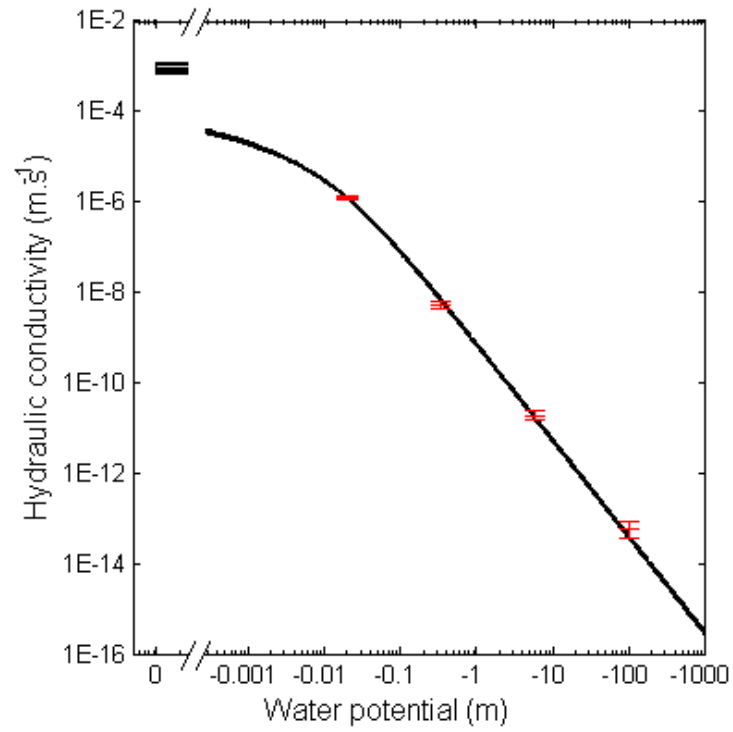
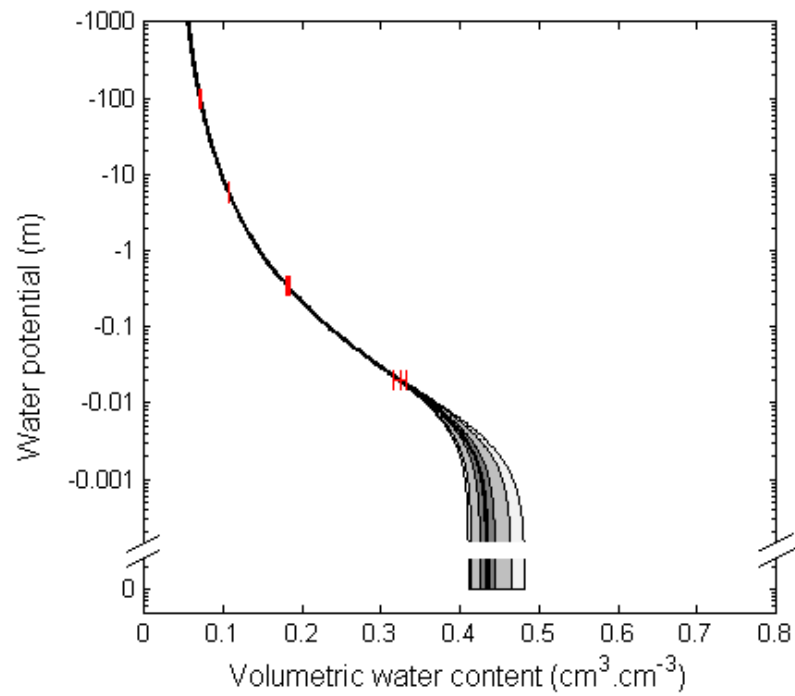


Figure 7

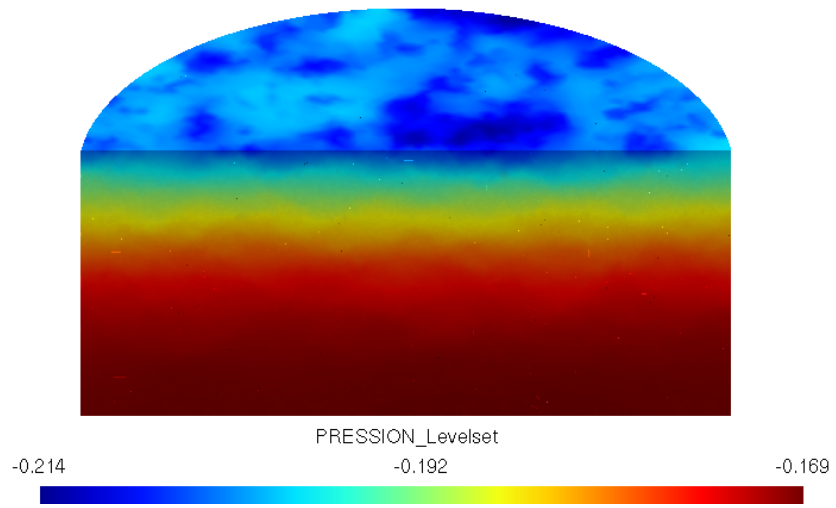


(a)

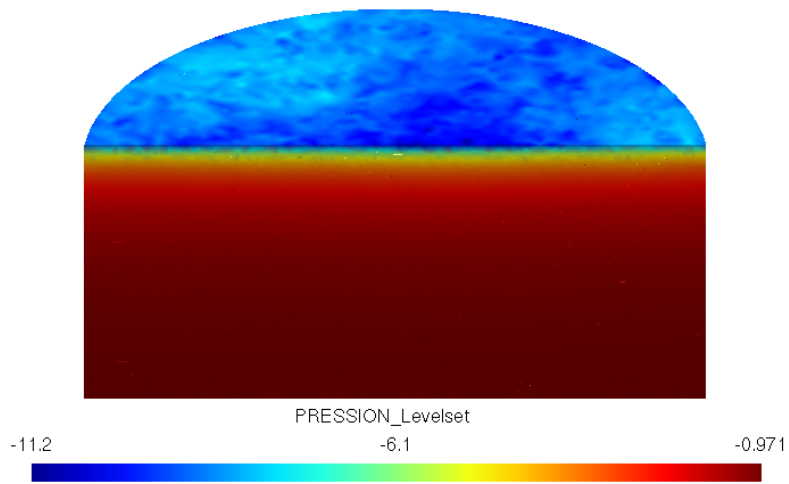


(b)

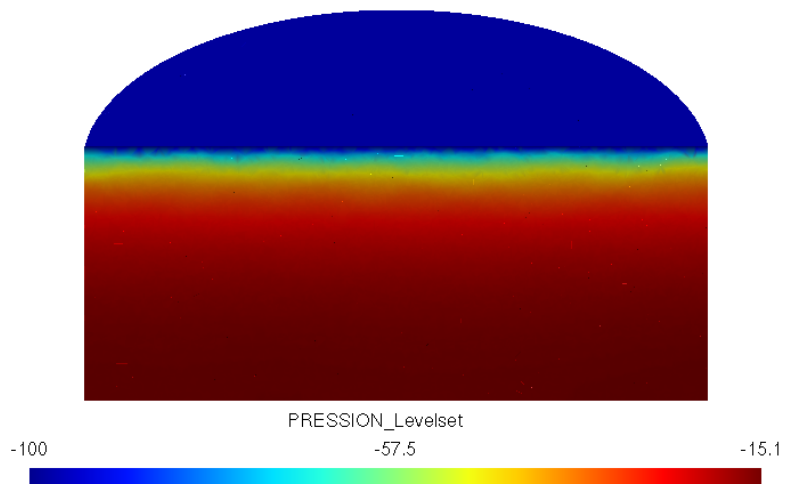
Figure 8



(a)



(b)



(c)

Figure 9

